

# BlockFUL: Enabling Unlearning in Blockchained Federated Learning

Xiao Liu, Mingyuan Li, Guangsheng Yu, Xu Wang, Wei Ni, Lixiang Li, Haipeng Peng, and Ren Ping Liu

**Abstract**—Unlearning in Federated Learning (FL) presents significant challenges, as models grow and evolve with complex inheritance relationships. This complexity is amplified when blockchain is employed to ensure the integrity and traceability of FL, where the need to edit multiple interlinked blockchain records and update all inherited models complicates the process. In this paper, we introduce Blockchained Federated Unlearning (BlockFUL), a novel framework with a dual-chain structure—comprising a live chain and an archive chain—for enabling unlearning capabilities within Blockchained FL. BlockFUL introduces two new unlearning paradigms, i.e., parallel and sequential paradigms, which can be effectively implemented through gradient-ascent-based and re-training-based unlearning methods. These methods enhance the unlearning process across multiple inherited models by enabling efficient consensus operations and reducing computational costs. Our extensive experiments validate that these methods effectively reduce data dependency and operational overhead, thereby boosting the overall performance of unlearning inherited models within BlockFUL on CIFAR-10 and Fashion-MNIST datasets using AlexNet, ResNet18, and MobileNetV2 models.

**Index Terms**—machine unlearning, federated learning, dag, blockchain.

## I. INTRODUCTION

### A. Background and Motivations

Various Federated Learning (FL) structures highlight the inherent property of models, where inheritance relationships between models are distinctly visible, including traditional FL [1]–[3], multi-layer FL [4], [5], multi-server FL [6], [7], and decentralized FL [8]–[10]. These diverse structures, where the intricate connections between models naturally form a directed acyclic graph (DAG), demonstrate the extensive relevance of model inheritance. To enhance the integrity and traceability of these models, Blockchained FL has emerged [11]–[13], featuring “certified-by-blockchain” capabilities to ensure that the lineage and updates of each model are verifiable and trustworthy.

While helping prevent FL models from being tampered with [14]–[16] and provides traceability [17]–[19], using blockchains stops the models from being rectified (when needed, e.g., some training data contains sensitive information or is later identified as questionable or contaminated). In

X. Liu, M. Li, L. Li and H. Peng are with Beijing University of Posts and Telecommunications, China. E-mail: {liuxiao68, henryli\_i, lixiang, peng-haipeng}@bupt.edu.cn

G. Yu and W. Ni are with Data61 CSIRO, Sydney, Australia. E-mail: {saber.yu, wei.ni}@data61.csiro.au

X. Wang and R. P. Liu are with the Global Big Data Technologies Centre, University of Technology Sydney, Australia. E-mail: {xu.wang, renping.liu}@uts.edu.au

addition, any user is entitled to request to eliminate the impact of its personal training data on machine learning models [20], [21]. In this sense, machine unlearning [22]–[26] and the capability of editing and updating blocks in Blockchained FL systems [27]–[31] become relevant.

An advanced one among existing machine unlearning methods is Sharded, Isolated, Sliced, and Aggregated (SISA) [22], which divides data into independent slices and trains them separately. Only the affected model slice needs to be re-trained to improve unlearning efficiency. Unfortunately, the inheritance relationships among models prevent SISA unlearning from being executed in parallel. This is due to the nature of incremental learning, where knowledge is inherited along with the reference between models. This nature renders SISA incapable of isolating unlearning processes since models need to be broadcast to all clients in any round [32]–[36]. With SISA ruled out, alternatives such as re-training [20], [37]–[41] and gradient ascent [42]–[44] come to the fore. Re-training uses an updated dataset to re-train the entire model. Gradient ascent adjusts the model weights to generate larger errors on known data, thereby reducing its reliance on previously learned content and achieving “forgetfulness”.

Integrating blockchains with FL under model inheritance relations can incur significant overhead in the unlearning processes. One reason is that although primitives, such as the Chameleon Hash (CH), have been considered for conditionally editing blockchains [45], [46] at non-negligible costs with complex operations, historical models are recorded on-chain for certification purposes throughout iterations. Unlearning may require editing multiple related blockchain records to remove just one class of knowledge, which significantly increases the complexity of the unlearning operations. Another reason arises from the model inheritance, where a child model inherits and extends its parent model’s characteristics, structure, and parameters. When performing an unlearning operation, the requested model and all its child models need to be updated. To this end, two critical Research Questions (RQs) need to be addressed.

- **RQ1:** *How can a Blockchained FL framework unlearn historical models while mitigating the non-negligible costs of frequent blockchain edits and updates to all inherited models in FL systems?*
- **RQ2:** *What unlearning methods can be adapted in a Blockchained FL system, and what are their associated performance and costs?*

In response to these two RQs, we propose a new framework, named BlockFUL, to empower Blockchained FL with

unlearning capability. In this framework, users can delete data that they wish to remove or deem questionable, and update their models at an acceptable cost, without compromising the immutability of the blockchain, affecting the utility of inherited models, or altering their network structure.

## B. Contributions

This paper presents a novel Blockchain Federated Unlearning (BlockFUL) framework, which ensures model inheritance within generic FL systems and supports effective unlearning without compromising model interrelationships. BlockFUL features a dual-chain architecture—comprising a live chain and an archive chain—to provide users with appropriate access for unlearning. Designed for flexibility, BlockFUL supports a plug-and-play approach. For illustration purposes, primitives such as CH and gradient ascent are considered in this paper. Nevertheless, CH and gradient ascent can be readily substituted with alternative redactable blockchain technologies and unlearning methods, such as re-training.

The contributions of this paper are summarized as follows:

- We introduce BlockFUL, the first comprehensive framework enabling unlearning within Blockchain FL. This framework features a dual-chain structure: an archive chain for storing all historical models, and a live chain that securely shares the latest updates and supports flexibility across any redactable blockchain method, including widely used CH-based technologies. BlockFUL mitigates the impact of model updates on inherited models, ensuring the traceability and integrity of FL models during unlearning tasks.
- We introduce two unlearning paradigms specifically considered in BlockFUL: parallel unlearning and sequential unlearning. These approaches facilitate the optimization of multiple model unlearning tasks within Blockchain FL, enabling the simultaneous update of multiple transactions and blocks via a single consensus operation. This strategy reduces the frequency of interactions between the FL and blockchain, and alleviates the burden on consensus operations.
- We comprehensively evaluate the effectiveness of BlockFUL by implementing two prevalent unlearning methods paired with the paradigms: parallel unlearning with gradient ascent, and sequential unlearning with re-training. Our analysis confirms that parallel unlearning effectively reduces dependency on data slated for unlearning and converges reliably. Additionally, we assess the overhead of CH and block update operations and compare the computational and communication costs associated with each method, providing a holistic view of their efficiency and practicality.

Experimental results confirm that sequential unlearning with re-training is highly effective. The model, after unlearning, achieves nearly zero accuracy for data meant to be unlearned and an accuracy of 94.71% for retained data across various models and datasets while maintaining model inheritance. However, this method can be time-intensive for models with deep inheritance chains and requires full participation from

all involved clients. In contrast, parallel unlearning with gradient ascent shows varied effectiveness based on different models and inheritance depths—the levels of hierarchical dependencies within the inheritance DAG among models, with results including 1.67% unlearning effectiveness in AlexNet and 77.67% for retained data.

## C. Paper Organization

The rest of this paper is organized as follows. The related works are reviewed in Section II. The proposed BlockFUL framework is provided in Section III. The designed dual-chain architecture is presented in Section IV, followed by two unlearning paradigms in BlockFUL introduced in Section V. Section VI presents the comparative experiments between the gradient ascent and re-training methods implemented in the new BlockFUL framework. Section VII concludes this work.

## II. RELATED WORK

Existing federated unlearning (FUL) research has been focused primarily on parameter adjustment and re-training processes. For instance, Halimi et al. [20] reversed a learning process by training the model to maximize local empirical losses, and executed deletion of client contributions using Projected Gradient Descent (PGD) at clients. Wu et al. [43] utilized class disassociation learning, client disassociation learning, and sample disassociation learning, and utilized reverse Stochastic Gradient Ascent (SGA) and Elastic Weight Consolidation (EWC) for joint unlearning of these three types of requests. FedEraser [37] utilized the historical parameter updates re-trained by the central server during FL to reconstruct the unlearning model. Wu et al. [47] eliminated client contributions by subtracting accumulated historical updates from the model, and utilized knowledge distillation methods to restore model performance without using client data. FRU [21] eliminates user contributions by rolling back and calibrating historical parameter updates, and then utilizes these updates to accelerate federated recommendation reconstruction. KNOT [48] introduces cluster aggregation and formulates the client clustering problem as a dictionary minimization problem for re-training processes. Liu et al. [41] utilized first-order Taylor expansion approximation techniques to customize a diagonal empirical Fisher information matrix-based fast re-training algorithm. FFMU [49] utilizes nonlinear function analysis techniques to refine local machine unlearning models into output functions of Nemytskii operators, maintaining unlearning quality while improving efficiency. Wang et al. [50] utilized CNN channel pruning to remove information about specific categories from the model for FUL processes.

Existing FUL studies predominantly assess whether the latest model version has been successfully unlearned, often overlooking crucial security challenges in FUL systems, such as trustworthiness, version control, and the traceability and accountability of unlearning iterations. They have not adequately addressed scenarios involving blockchain integration, where the need for tamper-proof data integrity and traceability introduces significant system overhead. These oversights become particularly problematic when integrating *certified-by-blockchain* with *model inheritance* across various prevalent

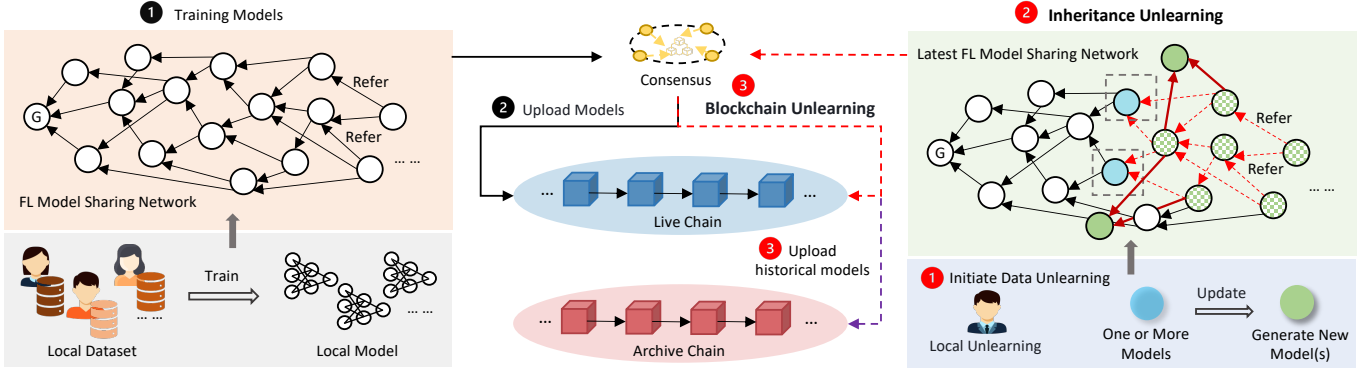


Fig. 1: This diagram summarizes BlockFUL. The existing training stage is illustrated on the left: Users (both clients and servers) participate in an FL task, where they reference existing models to generate models and publish them to the network. The models are uploaded to a blockchain-based storage system. The proposed unlearning stage is illustrated on the right: A user needs to unlearn data (blue node, one or more models) and update models (green nodes), triggering a cascade of updates to subsequent affected models (green lattice nodes), forming a sub-DAG of the inheritance relationship. Historical model records are maintained in the “archive chain” of a new dual-chain structure, while the model is up-to-date in the “live chain” of this dual-chain structure.

FL structures, as this combination significantly amplifies the complexity and cost of FUL processes. To this end, our proposed framework, BlockFUL, is the first to enable unlearning capability in Blockchain FL settings, addressing both the unique challenges of model inheritance and the additional overhead incurred during blockchain operations.

### III. SYSTEM MODEL

In this section, we describe the proposed BlockFUL framework, with unlearning capabilities in Blockchain FL. BlockFUL features a new dual-chain structure—comprising a live chain and an archive chain—to provide users with appropriate access for unlearning. BlockFUL ensures model inheritance within various FL structures and supports effective and efficient unlearning with comparable operations costs. Table I summarizes the notation.

#### A. Preparation

**Registration.** Before the users can participate in the BlockFUL task, they need to register in the network. The users are both model publishers and model users.

**Key initialization.** Each user generates two key pairs, i.e., the conversation key pair  $(pk, sk)$  and the CH key pair  $(CH_{pk}, CH_{sk})$ .

**Key usage and permissions.**  $pk$  and  $sk$  are used for signing and verifying a user’s legitimate identity. The CH private key  $CH_{sk}$  is assigned to a committee. As a result, the committee can participate in the redactable process of the blockchain. Meanwhile, the CH public key  $CH_{pk}$  is broadcast in the network. The users only have permission to share and use the model, and cannot perform change operations.

#### B. Training Models

As shown in Fig. 1, the BlockFUL framework is constructed based on an inheritance structure [51], where multiple users participate in FL training for a task, and each user can train multiple models. Consider a weighted directional graph

TABLE I: Notation and definition

Notation	Definition
$Tx_{i,j}$	The $j$ -th transaction of the $i$ -th block
$CH(i,j)$	The CH value in $Tx_{i,j}$
$v(i,j)$	The random number in $Tx_{i,j}$
$URI_w(i,j)$	The model identifier in $Tx_{i,j}$
$R_{Tx}(i,j)$	A list of transactions referenced by $Tx_{i,j}$
$\mathcal{T}(i,j)$	The payload contains $URI_w(i,j)$ and $R_{Tx}(i,j)$
$w_s$	The starting model of to-be-unlearned data in FL
$\nabla\theta_s$	Gradient of $w_s$ update
$w_y$	An inheritance model of $w_s$
$P$	The set of paths from $w_s$ to $w_y$
$w_j$ on $p_i$	Traverse the $j$ -th model on the $i$ -th path except $w_s$
$N^{R_j}$	The number of models referenced by $w_j$
$\nabla\theta_s^k$	Gradient of the $k$ -th starting model $w_s$ update
$p_i^{\nabla\theta_s^k}$	The $i$ -th path with gradient $\nabla\theta_s^k$
$P^{\nabla\theta_s^k}$	The set of paths with gradient $\nabla\theta_s^k$
$d_i$	The depth of path $p_i$
$W$	The set of starting updated models
$N(W)$	The set of models that inherit from $W$
$N^i(W)$	The set of $i$ -hop inherited models of $W$
$C_{tran}$	Transmission cost for uploading or downloading models
$C_{con}$	Consensus cost
$C_{CH}$	CH update cost

$G = (V, E)$ , where  $V = (GV, MV)$ . Herein,  $GV$  denotes the creation model node from which a task is issued, and  $MV = \{mv_1, mv_2, \dots, mv_j\}$  collects model nodes in the network that participate in an FL task. The weighted edges, collected by  $E = \{e_{01}, e_{10}, \dots, e_{xx}\}$ , represent the links of inheritance relationship between the user models in the network.

Non-existent links indicate that the weights are null. The inheritance relation,  $r_{j \rightarrow s} = \{mv_j \rightarrow mv_s\}$ , indicates that  $mv_j$  inherits from  $mv_s$ . Moreover,  $R_j = \{r_{j \rightarrow s}, r_{j \rightarrow f}, \dots\}$  denotes the set of inheritance relationships referencing other model nodes from  $mv_j$ . It is further expressed as  $\mathbb{R}_{j \rightarrow \dots \rightarrow s} = \{R_j, \dots\}$ , as shown in Fig. 2. Here,  $r_{j \rightarrow s}$  is one of the

elements in the set of the weighted edges,  $E$ .

1) *Candidate models*: A user employs its local test dataset  $D^{test}$  to randomly select a number of models contributed by the other users for evaluation. Subsequently, the user obtains the test accuracy set  $AC^{test}$  of these models until collecting  $K$  candidate model sets  $W^*$ , as given by

$$(AC^{test}, W^*) = \{(F(w_i, D^{test}), w_i) \mid w_i \in K, \\ i = 1, 2, \dots, k\}, \quad (1)$$

where  $F(\cdot)$  indicates that the user evaluates the model on its own test dataset  $D^{test}$  using the model  $w_i$  and obtains an accuracy. Then, this function  $F(\cdot)$  returns the accuracy value.

2) *Selection and aggregation*: The user selects the top- $N$  models from the previous randomly selected  $K$  candidate models, which constitute a referenced model set  $\mathbb{N}$  for accuracy ranking. Then, the user conducts model aggregation to obtain a pre-aggregation model  $\tilde{W}$ , as given by

$$\tilde{W} = \sum_{w_n \in \mathbf{w}} \frac{1}{N^{R_n}} w_n, \quad (2)$$

where  $\mathbf{w}$  is the set of models in the referenced model set  $\mathbb{N}$  and  $N^{R_n}$  is the number of referenced models associated with model  $w_n$ .

3) *Training*: The user trains  $\tilde{W}$  with its local training dataset  $D^{train}$  to obtain the final aggregated model  $W$ :

$$W = \Upsilon(\tilde{W}, \phi, D^{train}), \quad (3)$$

where  $\phi$  denotes the training settings, including the learning rate and batch size; and  $\Upsilon(\cdot)$  denotes the user's training function for the task.

4) *Evaluation*: After the completion of training, the user evaluates the model on its local test dataset  $D^{test}$  for the final accuracy  $AC$ .

5) *Node generation*: The user prepares a model node  $mv_j$  that includes the accuracy set  $\mathbb{AC}$  and the model set  $\mathbb{W}$  from the referenced model set  $\mathbb{N}$ , the CH value  $CH(W)$  of the model, the identifier  $URI(W)$  of the model,  $AC$ ,  $\phi$  and the creation timestamp  $T_{mv_j}$ . Then, user  $j$ ,  $\forall j$ , signs  $mv_j$  and broadcasts the signed nodes in the network.

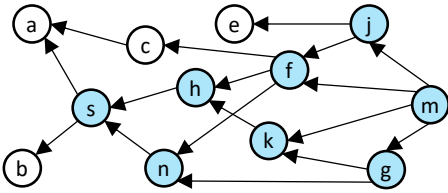


Fig. 2: The blue nodes are inherited nodes influenced by node  $s$ , namely, the child nodes of  $s$ .  $w_*$  represents the model corresponding to node  $*$ . Between  $w_s$  and  $w_m$ , the models affected by model  $w_s$  are  $w_n, w_h, w_k, w_f, w_j$  and  $w_g$ . Therefore, the set of inheritance relations  $\mathbb{R}_{m \rightarrow \dots \rightarrow s} = \{R_m, R_g, R_j, R_f, R_k, R_h, R_n\}$ .

### C. Unlearning Models

An unlearning process refers to scenarios where users participating in an FL task, if the training data later triggers

privacy concerns or is publicly identified as damaged, a part of the training data needs to be withdrawn according to regulations such as GDPR [52]. Unlearning tasks are employed to remove this data's influence from the models, ensuring that previously trained models can no longer recognize such data. In BlockFUL, this unlearning process needs to be conducted across the inheritance DAG, followed by an additional blockchain unlearning process.

1) *Inheritance unlearning phase*: The unlearning request is initiated by a specific node. Employing various unlearning methods, all inherited models influenced by this node need to be updated, as shown by the green lattice nodes in Fig. 1. The updating process continues until the model nodes reach the latest generated nodes. Two cases are studied in Section V.

2) *Blockchain unlearning phase*: As described in Section IV-A, we design the block structure in the live chain. Each transaction has a transaction reference list  $R_{Tx}$  to record the reference relations of its transactions. Based on these relations, we can obtain the entire inheritance model network structure, which allows all inherited transactions to be updated comprehensively.

### D. Player Model

**User.** Two assumptions of user behaviors are considered. First, model inheritances are time-sensitive. New users joining the FL task cannot train with models from before a certain block height. Second, all users participating in the FL task are considered *honest-but-curious*. Users honestly follow the procedures, which grant them access only to the live chain to retrieve the latest model versions. Users are then curious about inferring sensitive training data from these models, which is effectively mitigated by executing the unlearning process.

**Adversary.** Attackers refer to external malicious entities who do not contribute to the Blockchain FL [53], [54] and could alternatively attempt to disrupt the blockchain consensus by gaining control of more than the faulty threshold from the committee. This risk can be mitigated by prevalent committee election mechanisms powered by reliable pseudo-random generators used in advanced consensus algorithms or sharding technologies [55].

**Committee.** The committee consists of users elected to validate transactions and maintain the network's integrity. While members are expected to adhere to protocol specifications to prevent fraud, the system can withstand a fraction of its members being compromised; exceeding this fraction may result in failed validations and security breaches, threatening the reliability and effectiveness of the Blockchain FL process.

### E. Design Goal

Our goals for unlearning in Blockchain FL include:

**G1. Unlearning effectiveness.** Unlearning effectiveness is defined by the system's ability to completely eliminate the impact of unlearned data on the model. An effective unlearning process guarantees the data samples that have been unlearned no longer affect the model's predictions or parameters.

**G2. Comparable model utility.** The unlearning scheme should preserve the model accuracy on retained data categories across all updated models in the DAG of the model inheritance. This requires careful design to ensure that the unlearning process does not adversely affect the overall performance of the models and the utility of the retained data.

**G3. Support multi-start and multi-class unlearning.** The unlearning process can start with multiple models in the DAG. This scenario arises when a user contributes multiple models to the FL task within a period and requests unlearning from all contributed models. The unlearning tasks are expected to unlearn a single or multiple classes of data.

**G4. Manageable unlearning cost.** The resource and time overhead of running unlearning tasks should be reasonable and feasible. In the case of unlearning tasks with multiple starting models, the costs of unlearning with multiple starts should be substantially lower than the total cost of unlearning with individual starts.

#### IV. PROPOSED DUAL-CHAIN UNLEARNING ARCHITECTURE

In this section, we design a new dual-chain structure in the BlockFUL framework, where an archive chain is utilized to record historical models and a live chain is employed to share the up-to-date FL models. We design the block structure in the live chain using primitives, such as the CH algorithm, to provide redactable operations on the data stored on the live chain to enable the process of the blockchain unlearning stage.

##### A. Transactional Models in the Dual-Chain Structure

This process records models in the blockchain. In our dual-chain structure, each transaction represents a model, and each block contains multiple transactions. These transactions are uploaded to the archive and live chains separately, through unified consensus, thereby reducing the frequency of the consensus process in the entire blockchain network. Models are stored in the Inter Planetary File System (IPFS) after undergoing consensus and validation. Note that the models of the archive chain and the live chain are stored in different IPFS instances. Fig. 3 shows the proposed dual-chain structure.

**Archive Chain.** The block data records generated by local participation in FL are uploaded to the archive chain. The archive chain does not grant access permission to FL users; only relevant auditing parties can view model records in the archive chain when necessary. This approach provides traceability for all model uploading activities and ensures the integrity of the models. The archive chain needs to record all complete historical models before and after unlearning. These historical models do not need updating. In this case, a smart contract manages historical models in a list format.

**Live Chain.** The transaction records generated by local training models are uploaded to the live chain. The live chain provides model sharing and includes the latest model versions. Model updates are executed by the committee. The models are only updated on the live chain when all committee members reach a unanimous consensus. The structure of the live chain

differs from that of the archive chain. Since the live chain only records the latest state of the models, smart contracts need to operate with models as transaction entries.

In the live chain, we design the structure of the blockchain to link our blocks by having the hash of the current block's parent point to the hash of the previous block. Each block consists of a block header and a block body, consistent with the structure of traditional blocks. We use CH to ensure that transactions and block headers are redactable. This design enables BlockFUL to update multiple transactions and blocks simultaneously through a single committee consensus operation, reducing consensus frequency.

**Block header.** Fig. 3 shows a block with height  $H$ . The block header contains the following key fields.

- $H_p(h)$ : This is the parent hash of the block before linking.
- $CH_{curr}(h)$ : Considering a model update task, it functions as the hash value for the current block. This role ensures that any changes to the model version resulting from updates, do not affect the validity of the current block.
- $R_{curr}(h)$ : The latest random number for the version-based CH value.
- *version*: This field is updated with the corresponding version number for each update task, maintaining consistent versions in the global state.

There are also the common block body's Merkle root  $MR(h)$  and the current block generation time *timestamp* in the block header.

**Block body.** A block body contains multiple redactable transactions uniformly composed in a Merkle tree structure and stores model-related values. A redactable transaction contains the following fields, where, we take transaction  $Tx_{i,j}$  as an example, i.e., the  $j$ -th transaction in the body of block  $i$ .

- CH Value  $CH(i,j)$ : This is the CH value of a transaction, and the field remains unchanged because it is involved in the  $MR(h)$  calculation.
- Model  $URI_w(i,j)$ : This field stores the identifier of the model linked to the transaction. Only one model identifier is recorded per transaction. According to  $URI_w(i,j)$ , we can find the corresponding model in the IPFS.
- Random Number  $v(i,j)$ : This field stores the latest random number used to compute the CH value based on  $URI_w(i,j)$ .
- $Tx_{i,j}$ 's reference list  $R_{Tx}(i,j)$ : This field stores the list of transactions with models referenced by the model stored in  $Tx_{i,j}$ . Based on all the reference lists stored in the blockchain, we can obtain the inheritance relations of all models in the BlockFUL task.

The design of this block contributes to efficient and secure redactability in the blockchain. Due to the use of CH, transaction updates do not alter the block body's Merkle root. However, the version field in the block header may cause collaborative updating issues with the block header. To ensure the consistency of transaction versions, we introduce the *version* field in the block body. As a result, the validity

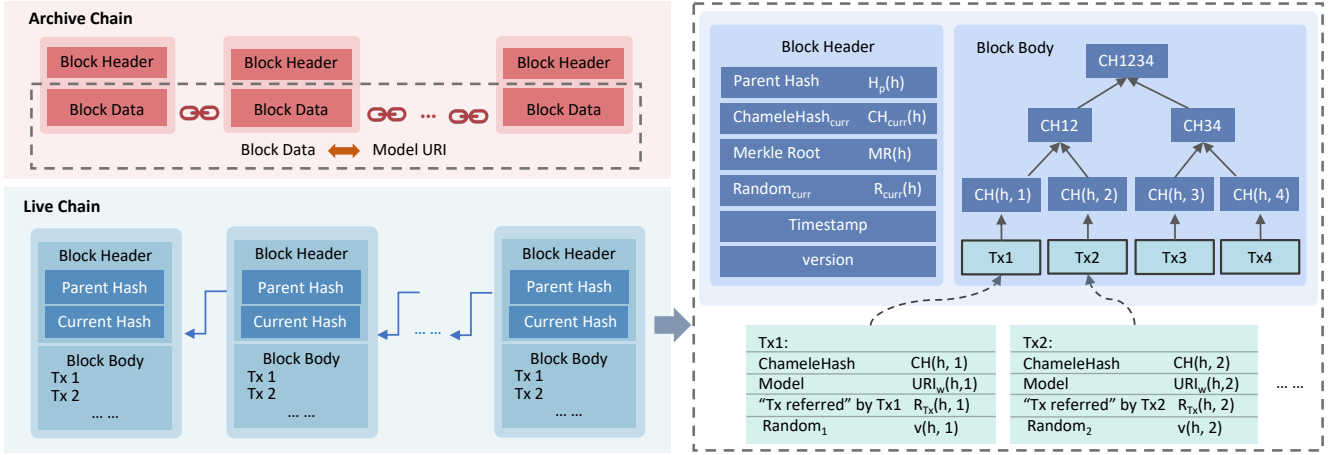


Fig. 3: In the dual-chain structure of BlockFUL, the archive chain stores the model’s URI as block data, with multiple block data entries included within a single block. Conversely, in the live chain, the model’s URI is embedded within individual transactions, with multiple transactions encapsulated in one block. Prior to any update triggered by an unlearning request, models scheduled for replacement are uploaded to the archive chain, followed by updates to the live chain that record the model in its latest version. This procedure is also applied to models undergoing multiple updates in one unlearning task.

of the link between blocks is maintained, and computational overhead is minimized.

Moreover,  $CH(i, j)$  is a field in the block that needs verification for the block body. In this way, even if  $URI_w(i, j)$  and  $v(i, j)$  are updated,  $CH(i, j)$  in the block body remains unchanged. Thus,  $MR(h)$  in the block header also remains unchanged. These conditions satisfy the immutability of  $CH_{curr}(h)$  and  $CH(i, j)$ . A valid block with an immutable block header can still be verified.

On the other hand, this redactability does not compromise the tamper-resistance of the blockchain. The redactability of blocks is guaranteed by  $CH_{sk}$  (trapdoor), an indispensable input for CH updates [27]. Meanwhile, to prevent malicious committee members from deliberately exposing outdated transaction information, once a transaction becomes outdated, it is not stored, but directly discarded instead.

### B. Model Unlearning in the Live Chain

During the initialization phase, the CH public-private key pair is generated by the users participating in FL. We first generate a private (trapdoor) key  $CH_{sk}$  and a public (hash) key  $CH_{pk}$  based on a security parameter  $\lambda$  and a system parameter  $CH_{para}$ .  $CH_{pk}$  is broadcast to the network. The committee members in the blockchain each hold a  $CH_{sk}$ . Next, the computation involves the payload  $\mathcal{T}(i, j)$  containing the hash value of the model  $URI_w(i, j)$  and the reference list  $R_{Tx}(i, j)$ , CH public key  $CH_{pk}$ , and a random number to generate the CH value. The calculation is as follows:

$$\mathcal{T}(i, j) = \{URI_w(i, j), R_{Tx}(i, j)\},$$

$$CH \text{ Hash}(\mathcal{T}(i, j), CH_{pk}, v(i, j)) \rightarrow \text{ChameleonHash}. \quad (4)$$

The parameter update equation related to CH, as specified in (5), ensures that the original CH value remains valid after information updates. The committee inputs the original payload  $\mathcal{T}(i, j)$ , which includes the model  $URI_w(i, j)$  before the update, along with the new payload  $\mathcal{T}'(i, j)$  containing the

updated model  $URI'_w(i, j)$  and the unchanged reference list  $R_{Tx}(i, j)$ , the random number  $v(i, j)$  before the update, and the corresponding private key  $CH_{sk}$ . It outputs the updated random number  $v'(i, j)$ , as follows:

$$CH \text{ update}(\mathcal{T}(i, j), \mathcal{T}'(i, j), v(i, j), CH_{sk}) \rightarrow v'(i, j). \quad (5)$$

Finally, by replacing the updated payload  $\mathcal{T}'(i, j)$  and  $v'(i, j)$  in the original  $ChameleonHash$ , the output satisfies the following conditions:

$$CH \text{ hash}(\mathcal{T}'(i, j), CH_{pk}, v'(i, j)) =$$

$$CH \text{ hash}(\mathcal{T}(i, j), CH_{pk}, v(i, j)). \quad (6)$$

After the transaction update is completed, the block header also needs to be updated. This can be achieved by updating the version field, following a similar process to the transaction update. Once the committee’s consensus nodes complete the transaction and block updates, the committee sends the updates to the other consensus nodes to complete the entire consensus process.

## V. BLOCKCHAINED FEDERATED UNLEARNING PARADIGMS

In this section, we elaborate on the new parallel and sequential unlearning paradigms in BlockFUL and explain the implementation processes by applying gradient ascent and re-training, respectively. We present the algorithms and their computational costs. Note that gradient ascent and re-training do not serve as comparative baselines, but rather as implementations for realizing the two distinct unlearning paradigms of parallelism and sequentialism.

### A. Paradigm 1 - Parallel Unlearning

In this paper, “parallel unlearning” refers to the committee members collectively reaching a single consensus for updating all to-be-unlearned models within an unlearning task. After

updating all models and reaching a unified consensus, the results are recorded on the chain simultaneously. To illustrate the parallel unlearning paradigm, we employ the gradient ascent to demonstrate this process. We introduce a new gradient passing function that manipulates the ascending gradients for inherited models within the DAG using the ascending gradients from the starting models. Then, the inherited models can be updated in parallel using the generated ascending gradients. In the function design, we prioritize the unlearning results across all inherited models by highlighting the inheritance relationships from the starting models to the inherited models.

**Update with a single starting model.** In this case, multiple paths may exist from the starting model to an inherited model. The update of the inherited model depends on the model nodes traversed by these paths and the number of models they inherit.

A user requesting to-be-unlearned data, re-trains the original model  $w_s$  on its client to generate an updated model  $w'_s$ . The difference between the gradients of the model before and after unlearning the data can be obtained, denoted by  $\nabla\theta_s$ . Starting from the updated model  $w'_s$ , an inherited model  $w_y$  of the original model  $w_s$  could be updated accordingly as

$$w'_y = \sum_{p_i \in P} \frac{1}{\prod_{w_j \text{ on } p_i} N^{R_j}} \times \alpha \nabla\theta_s + w_y, \quad (7)$$

where  $P$  denotes the set of paths from  $w_s$  to  $w_y$ ,  $P = \{p_1, \dots, p_l\}$ , “ $w_j$  on  $p_i$ ” denotes traversing each model node on path  $p_i$  except  $w_s$ ,  $N^{R_j}$  denotes the number of models inherited by model node  $w_j$  passing through path  $p_i$ , and  $\alpha$  denotes discount factor. Equation (7) handles model inheritance in FL, enabling the update of all relevant inherited models.

**Update with multiple starting models.** In this case, a user participating in a BlockFUL task contributes multiple models, and these models may have different gradients. During updates, these models serve as the starting models and have varying degrees of influence on the inherited models (i.e., the update of the inherited models may involve the computation of one or more starting model gradients). In other words, the inherited models may be affected by scenarios, for example, the same gradient but different paths, or different gradients and different paths.

For a model  $w_y$  affected by multiple starting model updates, the update results are given by

$$w'_y = \sum_{\substack{\nabla\theta_s^k \in \nabla\theta \\ P^{\nabla\theta_s^k} \in \mathbb{P}}} \left( \sum_{p_i^{\nabla\theta_s^k} \in P^{\nabla\theta_s^k}} \frac{1}{\prod_{w_j \text{ on } p_i} N^{R_j}} \times \alpha \nabla\theta_s^k \right) + w_y, \quad (8)$$

where  $\nabla\theta$  denotes the set of multiple model gradients for a user, and  $\nabla\theta = \{\nabla\theta_s^1, \nabla\theta_s^2, \dots, \nabla\theta_s^h\}$ ;  $p_i^{\nabla\theta_s^k}$  denotes the  $i$ -th path with gradient  $\nabla\theta_s^k$ , and  $P^{\nabla\theta_s^k}$  denotes the set of paths with gradient  $\nabla\theta_s^k$ . Additionally,  $\mathbb{P}$  is the set of paths with all gradients, i.e.,  $\mathbb{P} = \{P^{\nabla\theta_s^1}, \dots, P^{\nabla\theta_s^h}\}$ .

The gradient ascent process continues on inherited models until a threshold  $\varepsilon$  is reached, beyond which a model  $w_y$  is not updated if  $|w'_y - w_y| \leq \varepsilon$ . If the FL training task ends before

reaching the threshold, the parallel gradient ascent process also stops. As shown in (7) and (8), the updated model  $w'_y$  is related to the number of model inheritances along the path from the starting models to model  $w_y$ . Furthermore, the number of model inheritances is associated with the depth from the starting models to model  $w_y$ . As the gradient ascent process carries on, a larger number of model inheritances leads to a faster reduction in the gradients and shallower updates.

Next, we prove the depths required from the starting model to its inherited model to cease updating are bounded. By denoting  $\nabla\theta$  as  $\alpha \nabla\theta_s$ , and considering  $D = \{d_1, d_2, \dots, d_l\}$  with  $d_i$  being the depth of path  $p_i$ , we have the following theorem.

**Theorem 1.** *When the number of model inheritances is  $N^{R_j} \geq 2$ , the depth required for model updating to complete satisfies*

$$d_i \geq \lceil \log_2 \frac{|\nabla\theta|}{\varepsilon} \rceil, \quad \forall d_i \in D; \quad (9)$$

$$\sum_{d_i \in D} \frac{1}{2^{d_i}} \leq \frac{\varepsilon}{|\nabla\theta|}. \quad (10)$$

*Proof.* First, from (7), it readily follows that

$$|w'_y - w_y| = \sum_{p_i \in P} \frac{1}{\prod_{w_j \text{ on } p_i} N^{R_j}} \times |\nabla\theta| \leq \varepsilon. \quad (11)$$

As discussed earlier, on a path  $p_i$ ,  $w_s$  passes through multiple model nodes to reach model  $w_y$  with depth  $d_i$ . The number of inheritances per model is  $N^{R_j} \geq 2$ , with the corresponding  $\frac{1}{N^{R_j}} \leq \frac{1}{2}$ . For this path  $p_i$ , we have

$$\frac{1}{\prod_{w_j \text{ on } p_i} N^{R_j}} \leq \frac{1}{2^{d_i}}. \quad (12)$$

Further, after passing through several model nodes,  $w_s$  arrives at a model of depth  $d_i$ , yielding

$$\frac{|\nabla\theta|}{\prod_{w_j \text{ on } p_i} N^{R_j}} \leq \frac{|\nabla\theta|}{2^{d_i}} \leq \varepsilon. \quad (13)$$

For path  $p_i$ , we have

$$2^{d_i} \geq \frac{|\nabla\theta|}{\varepsilon} \implies d_i \geq \lceil \log_2 \frac{|\nabla\theta|}{\varepsilon} \rceil. \quad (14)$$

For a set  $P$  of all paths, we have

$$\begin{aligned} \sum_{p_i \in P} \frac{|\nabla\theta|}{\prod_{w_j \text{ on } p_i} N^{R_j}} &\leq \sum_{d_i \in D} \frac{|\nabla\theta|}{2^{d_i}} \leq \varepsilon \\ \implies \sum_{d_i \in D} \frac{1}{2^{d_i}} &\leq \frac{\varepsilon}{|\nabla\theta|}. \end{aligned} \quad (15)$$

If  $\frac{1}{\prod_{w_j \text{ on } p_i} N^{R_j}} = \frac{1}{2^{d_i}}$  at this point, the value of  $d_i$  can be obtained as

$$d_i = \begin{cases} 1, & \text{if } \log_2 \left( \frac{|\nabla\theta|}{\varepsilon} \right) < 0; \\ \lceil \log_2 \frac{|\nabla\theta|}{\varepsilon} \rceil, & \text{if } \log_2 \left( \frac{|\nabla\theta|}{\varepsilon} \right) \in \mathbb{R}^+ \setminus \mathbb{Z}^+. \end{cases} \quad (16)$$

Theorem 1 is proved.  $\square$

As dictated in Theorem 1, the minimum depth for completing a model unlearning task is determined by the variable

$\nabla\theta$ . Since  $\nabla\theta$  is finite, there must exist a depth bound  $d_b = \lceil \log_2 \frac{|\nabla\theta|}{\varepsilon} \rceil$  such that models after  $d_b$  do not need to be updated. When  $\nabla\theta$  is smaller, it requires smaller depths for the model to stop updating. On the other hand, if  $|\nabla\theta|$  is larger, it requires more depths for the model to stop updating. As mentioned earlier, the model update is related to  $N^{R_j}$ , while a bound of  $N^{R_j} = 2, \forall j$  is assumed in the proof. Therefore, when  $\nabla\theta_s$  remains constant, the larger  $N^{R_j}$  is, the smaller update depth bound is, and the smaller depths are required for the model to stop updating.

If there are model nodes that reference only one model for training throughout the FL training task, the depth at which the model stops updating is  $d + c$ . Here,  $c$  represents the number of nodes inheriting only one model.

**Corollary 1.** *When multiple models of a user are used as starting points for model update, and there are interactions between these inherited models affected by the starting models, these inherited models also stop updating at a certain depth.*

*Proof.* According to (8), assuming model  $w_y$  is influenced by multiple distinct gradient model updates, we can represent  $B_s^k$  the gradient ascent required for  $w_y$  under the influence of gradient  $\nabla\theta_s^k$ . Here,  $B_s^k = \sum_{p_i^{\nabla\theta_s^k} \in P^{\nabla\theta_s^k}} \frac{1}{\prod_{w_j \text{ on } p_i} N^{R_j}} \times \alpha \nabla\theta_s^k$ . Since multiple starting models are updated simultaneously, the gradient ascent process accumulates individual gradient ascent values. In other words,  $B = B_s^1 + B_s^2 + \dots + B_s^h$ . According to Theorem 1, the inherited models influenced by the starting models eventually stop updating when a certain depth is reached. Therefore, as  $\prod_{w_j \text{ on } p_i} N^{R_j}$  increases,  $B_s^k \leq \varepsilon$ , further resulting in  $B \leq \varepsilon$ .  $\square$

**Parallel unlearning in BlockFUL.** In Algorithm 1, the users broadcast the updated model message to the network. Upon receiving the message, the committee processes the starting updated model set  $W$  and its inherited model set  $N(W)$ . According to (8), the committee performs gradient ascent updates on the inherited models. Similarly, these updates need to be executed on the blockchain. Since the reference list  $R_{Tx}$  in each transaction provides reference relations for all transactions in the BlockFUL task. With the assistance of  $CH_{sk}$ , each committee member can overwrite all transactions and versions to be updated in the blockchain. In this parallel unlearning, we only need to perform one consensus operation to update FL and the blockchain. Based on all these previous updates, a unified hash value can be computed. This hash value is used to execute the consensus process, which helps prevent malicious committee members from making false updates.

### B. Paradigm 2 - Sequential Unlearning

In this paper, ‘‘sequential unlearning’’ refers to a process where committee members execute a consensus process for each individual model update, i.e., a single DAG node, within an unlearning task. After updating one model and reaching a consensus, the results are recorded on the chain before moving on to the next model update. In the sequential unlearning paradigm, we employ the re-training method to demonstrate

---

### Algorithm 1: Parallel unlearning (gradient ascent)

---

```

1 Define Receiver  $\leftarrow$  Sender.Send(Message);
2 // This transmission is secured by any
  private and encrypted channels, e.g.,
  TLS.
3 Input:  $G = (V, E)$ , start model set  $W'$ , start model
   $w'_i \in W'$ , model gradient set  $\nabla\theta$ , discount factor  $\alpha$ 
4 for  $w'_i$  to  $W'$  parallel do
5   Send model_update message( $w'_i$ );
6   // broadcast to the network.
7   for  $w_j$  to  $N(W)$  do
8      $w'_j \leftarrow$  Committee.Update( $w_j, \nabla\theta, \alpha$ );
9     // Update the model weights
      influenced with  $W'$  by (8).
10     $v'_{i,j} \leftarrow$  Committee.Overwrite( $\mathcal{T}(i, j)$ ,
11     $\mathcal{T}^l(i, j), v_{i,j}, CH_{sk}$ );
12     $R'_{curr} \leftarrow$  Committee.Overwrite(version,
13    new version,  $R_{curr}, CH_{sk}$ );
14  end
15 end
16 while Consensus do
17   Committee.Verify( $Hash(W', N(W')), v'_{i,j}, R'_{curr}$ );
18   if  $Hash(W', N(W'), v'_{i,j}, R'_{curr})$  is invalid then
19     alarm and exit updated blocks;
20     Update the corresponding parameters in IPFS;
21   end
22 end

```

---

this process. Here, the same user model settings are used as in gradient ascent. The re-training starts from the updated model  $w'_s$  and goes through all paths to the model  $w_y$ .

1) *Re-aggregation:* Based pre-aggregation in (2), the re-aggregation model is expressed as

$$\tilde{w}'_y = \frac{1}{N^{R_y}} W'_y, \quad (17)$$

where  $W'_y$  denotes the updated set of the original selected model weights.

2) *Re-training:* Based on training in (3), the users associated with these paths re-train the model on their own local clients. The inherited model  $w_y$  is updated accordingly as

$$w'_y = \mathcal{T}_y(\tilde{w}'_y, \phi_y, D_y^{train}). \quad (18)$$

**Sequential unlearning in BlockFUL.** The steps for model updating using sequential unlearning, i.e., the re-training method, are shown in Algorithm 2. In this process, the client first checks whether it is the starting model. If it is not the starting model, the client performs the operations of re-aggregation and re-training of its own model locally. Then, the client broadcasts the model update message to the network. The committee utilizes  $CH_{sk}$  in the blockchain to perform the same updating operations as described in Algorithm 1. Subsequently, consensus verification is conducted. Upon reaching a consensus, the committee updates the blocks and parameters accordingly in the IPFS. Finally, the committee sends model update messages to the next-hop clients for updating the one-hop inherited models  $N^1(W)$ , two-hop inherited models  $N^2(W)$ , and so on and so forth, where all these inherited models of different hops belong to  $N(W)$ .



**Algorithm 2: Sequential unlearning (re-training)**


---

```

1 Define All functions inherited from Algo. 1;
2 Input:  $G = (V, E)$ , start model set  $W'$ , start model  $w'_i \in W'$ 
3 for  $w'_i$  to  $W'$  do
4   for  $w_j$  to  $N(W)$  do
5     if  $w_j \neq w'_i$  then
6       Re-aggregation according to (17);
7       Re-training according to (18);
8     end
9     Send model_update message( $w'_i$ ); // broadcast
      to the network.
10     $v'_{i,j} \leftarrow$  Committee.Overwrite( $\mathcal{T}(i, j)$ ,  $\mathcal{T}'(i, j)$ ,
       $v_{i,j}$ ,  $CH_{sk}$ );
11     $R'_{curr} \leftarrow$  Committee.Overwrite(version,
      new version,  $R_{curr}$ ,  $CH_{sk}$ );
12    while Consensus do
13      Committee.Verify( $W'$ ,  $v'_{i,j}$ ,  $R'_{curr}$ );
14      if  $W'$ ,  $v'_{i,j}$ ,  $R'_{curr}$  is invalid then
15        alarm and exit
16        updated blocks;
17        Update the corresponding parameters in
18        IPFS;
19      end
20    end
21    Clients( $N^1(W)$ )  $\leftarrow$  model_update message( $W'$ );
      // Parallel transmission.
22 end
23 end

```

---

TABLE II: Comparison between the parallel and sequential unlearning. This includes  $L$  blocks and  $K$  models that need updating, CH update cost  $C_{CH}$ , consensus cost  $C_{con}$ , and transmission cost  $C_{tran}$  for uploading or downloading models. These costs are independent of the implementation of the unlearning methods.

Paradigm	Computation Cost	Update Role
Parallel	$(K + L)C_{CH} + C_{con} + 2KC_{tran}$	Committee
Sequential	$2KC_{CH} + KC_{con} + 2KC_{tran} + N^R(K - 1)C_{tran}$	Client

### C. Cost Analysis of Blockchain Operations

This subsection analyzes the computational overhead of parallel unlearning and sequential unlearning paradigms, as well as block updating on the live chain. The update is executed every time a node is traversed, regardless of whether or not unlearning has been performed on the node. The number of consensus processes varies based on the unlearning techniques used: a single consensus occurs in parallel unlearning, whereas multiple consensus are required in sequential unlearning. On the other hand, the computational overheads of different unlearning paradigms on the archive chain are unaffected by model updates.

Here, the transmission cost  $C_{tran}$  represents the cost associated with a single operation of uploading  $C_{tran}^{up}$  or downloading  $C_{tran}^{down}$  a model. The committee consensus cost is  $C_{con}$ . The cost of a single CH update operation is denoted by  $C_{CH}$ . Suppose that  $L$  blocks and  $K$  models need to be updated, including  $M$  starting models and  $(K - M)$  inherited models.

1) *Parallel Unlearning: CH cost.* The cost of CH includes the cost of transactions CH  $C_{CH}^{Tx}$ , and the cost of blocks CH

$C_{CH}^{block}$  in the blockchain. Therefore, the CH cost of parallel unlearning is

$$C_{CH}^{Pa} = KC_{CH}^{Tx} + NC_{CH}^{block} = (K + L)C_{CH}. \quad (19)$$

**Block consensus cost.** The committee executes the entire parallel unlearning process, enabling consensus to be reached for multiple transactions or blocks simultaneously. The consensus cost of parallel unlearning is given by

$$C_{con}^{Pa} = C_{con}. \quad (20)$$

**Transmission cost.** The transmission cost of the model is primarily incurred at the consensus nodes for uploading and downloading. Since the consensus nodes can perform uploading and downloading tasks in parallel, the transmission cost of the model is modeled as

$$C_{tran}^{Pa} = KC_{tran}^{up} + KC_{tran}^{down} = 2KC_{tran}. \quad (21)$$

2) *Sequential Unlearning: CH cost.* In this process, each transaction update requires one transaction CH and one block CH. The CH cost of sequential unlearning is

$$C_{CH}^{Se} = KC_{CH}^{Tx} + KC_{CH}^{block} = 2KC_{CH}. \quad (22)$$

**Block consensus cost.** Each model update requires one round of consensus. The consensus cost for sequential unlearning is

$$C_{con}^{Se} = KC_{con}. \quad (23)$$

**Transmission cost.** The transmission cost of the model primarily involves the uploading and downloading processes by local clients, as well as the downloading process by consensus nodes. Suppose that the average number of inheritances per model is  $N^R$ . The transmission cost for sequential unlearning is given by

$$C_{tran}^{Se} = KC_{tran}^{up} + N^R(K - 1)C_{tran}^{down} + KC_{tran}^{down} = 2KC_{tran} + N^R(K - 1)C_{tran}. \quad (24)$$

We compare the computational costs and role updates of the two paradigms in Table II. Sequential unlearning incurs higher costs than parallel unlearning. This is because, during model updates, sequential unlearning requires first reaching a consensus and then recording the result on the chain, before proceeding to the next model update. During this process, the costs arise primarily from consensus and transmission overhead. For a model, the computational consumption of its updates can be  $2C_{CH} + C_{con} + 2C_{tran} + N^R C_{tran}$ .

In the case of one transaction corresponding to one block and the case of multiple transactions corresponding to one block, the block update costs are denoted by  $SC_{block}$  and  $MC_{block}$ , respectively.

**$Tx$ -block.** One or more transaction updates go through CH overhead  $C_{CH}$ . Similarly, the main overhead is the same as the transaction overhead for one block or multiple block updates. Suppose that there are  $K$  model updates. The costs can be given by

$$SC_{block} = K(C_{CH}^{block} + C_{CH}^{Tx}) = 2KC_{CH}. \quad (25)$$

**Transaction-block.** In the case of multiple transactions corresponding to a single block, suppose there are  $K$  model updates, then the update cost in this block is

$$MC_{block} = C_{CH}^{block} + KC_{CH}^{Tx} = (K + 1)C_{CH}. \quad (26)$$

3) *Comparison:* Based on the comparison of these paradigms, the choice of updating entity significantly affects computational costs. If individual users perform updates, each must upload their updated model to the blockchain and inform the next user, necessitating consensus for each update and incurring transmission overheads. As the number of updated models outpaces the number of block updates, the cumulative cost of CH in the blocks surpasses that of collective updates managed by the committee. Conversely, entrusting the committee with model updates alleviates the computational load on clients. As the number of models increases, consensus and transmission costs are lower than when managed by clients, allowing the committee to focus more on overall system performance and cost efficiency.

## VI. EXPERIMENTS

In the experiment, we establish a testbed and assess the effectiveness of the above-mentioned two paradigms—parallel and single unlearning. We evaluate the impact of these paradigms on accuracy for both unlearned and retained labels, incorporating classic models, such as ResNet18 and MobileNetV2. We also evaluate the overhead of interacting with the dual-chain structure. This thorough analysis extends to measuring the time consumption during training and inference, providing insights into the trade-offs between unlearning effectiveness and model utility within the framework.

We align the parallel unlearning paradigm with the gradient ascent and the sequential unlearning paradigm with the re-training. This alignment is reasonable since each method aptly reflects the characteristics of its respective unlearning paradigm: re-training, which requires sequentially fetching and training each model, and gradient ascent, which facilitates parallel processing due to its on-off fetching capability from the blockchain.

### A. Evaluation Metrics

For illustration convenience, our experiment concentrates on class-level unlearning tasks, although BlockFUL is technically capable of supporting class-, client-, and sample-level unlearning, thanks to the broad compatibility of BlockFUL that supports various prevalent unlearning methods, such as re-training and gradient ascent [56]. We evaluate the model’s accuracy using the training datasets to assess its practicality in experiments. This method is reasonable, as it directly tests whether the removed information continues to influence the model and is a standard practice in the field [44], [57], [58].

**Accuracy on the unlearned dataset ( $AD_f$ ).** The accuracy of an unlearned dataset in the unlearned model ideally is close to zero. This aligns with **G1** by evaluating the success of unlearning through the model’s inability to predict labels corresponding to the unlearned dataset accurately.

**Accuracy on the retained dataset ( $AD_r$ ).** The accuracy of a retained dataset of the unlearned model. It is expected to be close to the performance of the original model. This aligns with **G2** by maintaining comparable accuracy on retained labels corresponding to the retained dataset.

**Cumulative unlearning time.** The cumulative time required for each model to unlearn labels during the training process in machine learning and deep learning.

### B. Datasets

The datasets utilized in the experiments are as follows:

**CIFAR-10.** This is a widely used dataset for image classification tasks in computer vision. It consists of 60,000 32x32 color images in 10 different classes, with 6,000 images per class. The dataset is split into 50,000 training and 10,000 testing images.

**Fashion-MNIST.** This is a commonly used dataset for image classification tasks, similar to MNIST but more complex. The dataset comprises ten fashion categories, each comprising 60,000 grayscale images with a dimension of 28x28 pixels. The training set contains 55,000 images, while the test set includes 10,000 images.

### C. The implementations of paradigms

In our study, each traversal triggers an “unlearning” at every node, regardless of whether it has been unlearned previously or not. We employ the following unlearning methods:

**Re-training.** We re-train the unlearning model with a dataset containing unlearned data and the derivative models influenced by the data. We remove unlearned data from this dataset and sequentially train the model using the remaining data according to the inheritance relation.

**Gradient ascent.** This involves the inheritance relation where models are uploaded by the users with unlearned data. For the initial unlearning models, we calculate the difference in the model gradient before and after unlearning. Subsequently, the inheritance models utilize this gradient difference for gradient ascent. By assessing these gradients, we gain insights into the impact of re-training on the downstream models, helping us understand the unlearning process.

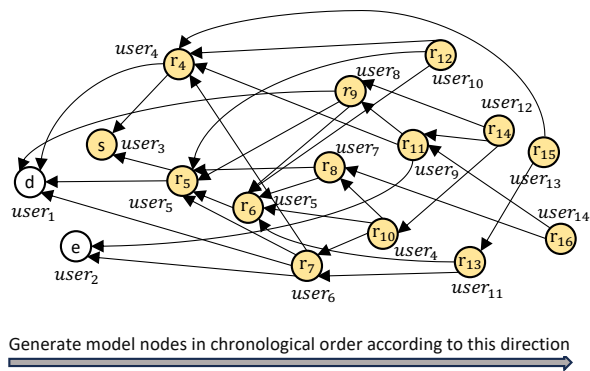


Fig. 4: The experiment considers 14 users, and each arrow represents the aggregated model. The yellow color indicates unlearned data models and their inheritance models.

TABLE III: Unlearning Performance on CIFAR-10

Model	# $C_f$	Metrics	Original Model			Re-training Model			Gradient Ascent			Cumulative Unlearning Time (s)					
			$r_5$	$r_6$	$r_8$	$r_5$	$r_6$	$r_8$	$r_5$	$r_6$	$r_8$	Re-training			Gradient Ascent		
												$r_5$	$r_6$	$r_8$	$r_5$	$r_6$	$r_8$
MobileNetV2	1	$AD_r \uparrow$	81.36%	71.44%	99.40%	79.92%	82.85%	96.83%	51.53%	44.59%	42.02%	181.09	361.77	596.89	28.32	29.9	31.28
		$AD_f \downarrow$	77.44%	77.04%	99.98%	0.00%	0.00%	0.00%	7.39%	8.52%	8.60%						
	2	$AD_r \uparrow$	98.56%	87.71%	82.49%	89.45%	78.76%	87.94%	53.64%	30.56%	17.56%	181.94	376.88	583.02	28.62	29.34	30.09
		$AD_f \downarrow$	79.40%	86.21%	78.42%	0.00%	0.00%	0.00%	8.00%	7.16%	5.54%						
	4	$AD_r \uparrow$	92.43%	86.99%	86.70%	86.15%	94.37%	94.84%	50.97%	35.80%	16.58%	151.14	311.59	471.64	28.66	29.98	32.98
		$AD_f \downarrow$	74.46%	74.11%	90.09%	0.00%	0.00%	0.00%	6.55%	9.36%	0.00%						
	7	$AD_r \uparrow$	92.30%	99.99%	97.39%	99.99%	99.99%	99.99%	99.29%	51.87%	52.99%	84.55	164.17	245.01	28.40	30.38	32.21
		$AD_f \downarrow$	90.15%	91.86%	91.68%	0.00%	0.00%	0.00%	8.75%	4.32%	7.90%						
ResNet18	1	$AD_r \uparrow$	99.99%	99.99%	89.25%	99.99%	95.85%	99.99%	60.64%	52.78%	54.95%	312.95	625.27	951.14	28.62	30.05	31.59
		$AD_f \downarrow$	99.99%	99.99%	92.73%	0.00%	0.00%	0.00%	7.76%	8.38%	6.78%						
	2	$AD_r \uparrow$	74.63%	90.09%	95.28%	99.99%	94.13%	91.95%	52.22%	60.17%	72.05%	290.76	597.86	907.71	28.67	29.8	31.03
		$AD_f \downarrow$	98.82%	90.43%	97.70%	0.00%	0.00%	0.00%	8.95%	5.23%	3.45%						
	4	$AD_r \uparrow$	80.08%	88.00%	99.87%	90.42%	98.54%	99.95%	41.83%	58.00%	63.92%	218.85	442.17	664.46	28.55	29.86	30.83
		$AD_f \downarrow$	89.21%	82.15%	99.68%	0.00%	0.00%	0.00%	4.50%	9.49%	8.50%						
	7	$AD_r \uparrow$	92.49%	90.19%	98.31%	99.95%	87.81%	99.99%	80.51%	54.49%	48.09%	134.04	264.57	391.35	28.54	30.66	32.27
		$AD_f \downarrow$	84.14%	81.98%	97.50%	0.00%	0.00%	0.00%	6.00%	8.52%	7.35%						

TABLE IV: Unlearning Performance on Fashion-MNIST

Model	# $C_f$	Metrics	Original Model			Re-training Model			Gradient Ascent			Cumulative Unlearning Time (s)					
			$r_5$	$r_6$	$r_8$	$r_5$	$r_6$	$r_8$	$r_5$	$r_6$	$r_8$	Re-training			Gradient Ascent		
												$r_5$	$r_6$	$r_8$	$r_5$	$r_6$	$r_8$
AlexNet	1	$AD_r \uparrow$	99.99%	99.99%	99.81%	99.99%	99.99%	98.80%	90.38%	84.36%	72.50%	43.57	84.85	126.45	27.72	27.98	28.15
		$AD_f \downarrow$	99.99%	99.99%	99.66%	0.00%	0.00%	0.00%	4.00%	3.99%	0.00%						
	2	$AD_r \uparrow$	99.99%	99.99%	99.80%	99.99%	99.99%	99.51%	81.71%	62.08%	74.26%	42.25	82.33	122.15	27.71	28.07	28.33
		$AD_f \downarrow$	99.99%	99.99%	99.49%	0.00%	0.00%	0.00%	0.00%	0.00%	5.00%						
	4	$AD_r \uparrow$	99.99%	99.99%	99.96%	99.99%	99.99%	99.16%	72.14%	66.52%	61.03%	40.34	77.65	115.51	27.71	28.51	28.91
		$AD_f \downarrow$	99.99%	99.99%	99.89%	0.00%	0.00%	0.00%	7.00%	0.00%	0.00%						
	7	$AD_r \uparrow$	99.99%	99.99%	99.72%	99.71%	92.72%	90.84%	90.16%	92.82%	84.03%	35.09	69.72	103.77	28.4	29.75	30.89
		$AD_f \downarrow$	99.99%	99.99%	98.82%	0.00%	0.00%	0.00%	0.00%	0.00%	0.00%						
ResNet18	1	$AD_r \uparrow$	99.90%	99.73%	94.10%	95.36%	83.35%	94.11%	82.35%	86.08%	84.69%	261.35	515.62	763.3	27.87	28.39	28.93
		$AD_f \downarrow$	99.99%	99.99%	94.49%	0.00%	0.00%	0.00%	0.00%	3.85%	6.27%						
	2	$AD_r \uparrow$	92.74%	92.74%	99.64%	95.67%	97.44%	91.37%	29.30%	64.45%	41.28%	236.34	465.44	697.74	28.03	28.77	29.42
		$AD_f \downarrow$	95.75%	95.70%	98.35%	0.00%	0.00%	0.00%	5.00%	5.22%	1.81%						
	4	$AD_r \uparrow$	95.77%	98.97%	98.48%	99.96%	98.43%	95.02%	45.46%	69.25%	51.18%	175.26	353.09	532.84	28.27	29.49	30.7
		$AD_f \downarrow$	62.73%	95.02%	99.71%	0.00%	0.00%	0.00%	9.75%	2.63%	0.12%						
	7	$AD_r \uparrow$	91.48%	87.32%	85.49%	92.59%	89.85%	98.61%	50.06%	32.05%	32.05%	115.51	223.26	330.35	28.56	30.67	32.72
		$AD_f \downarrow$	74.46%	89.32%	91.84%	0.00%	0.00%	0.00%	5.57%	0.00%	0.00%						

#### D. Experimental Settings

We conduct experiments using an NVIDIA GeForce RTX 3070 GPU. We employ an untrained ResNet18 model, MobileNetV2 model, and AlexNet model, all fine-tuned on specific datasets. The to-be-unlearned classes during the process are represented as # $C_f$ .

**Model Inheritance.** A group of 14 users is evaluated, as depicted in Fig. 4.  $user_5$  and  $user_7$  have the same unlearning labels. The models highlighted in yellow are those that demonstrate accuracy in unlearned data.

**Blockchain.** In the live chain, we use Byzantine Fault Tolerance (BFT)-based consensus to ensure data consistency and security. Additionally, we set the block packaging time to 15 seconds. This interval strikes a balance between transaction processing speed and network stability. Each block is sized at 1MB to ensure efficient network transmission and storage.

**Hyperparameters.** In both CIFAR-10 and Fashion-MNIST setups, each model undergoes rigorous training for 100 epochs with a learning rate of 0.005.

**Label categories.** In both CIFAR-10 and Fashion-MNIST, we apply the unlearning process to both single category labels and multiple-category labels (including combinations of 2, 4, and 7 category labels). Here,  $r_5$ ,  $r_6$ , and  $r_8$  represent the models randomly targeted for the unlearning process.

#### E. Evaluating Unlearning Performance

We evaluate the performance of re-training and gradient ascent by comparing their results for  $AD_f$  and  $AD_r$ , which align with design goals **G1** and **G2**, respectively. We also assess unlearning performance across single and multiple class scenarios to meet design goal **G3**.

We present the results in Table III for the CIFAR-10 dataset and in Table IV for the Fashion-MNIST dataset. With the Fashion-MNIST dataset, we use AlexNet for prediction. It can be observed that AlexNet’s re-training time is much shorter than that of ResNet18. This suggests that in the case of models with fewer parameters, the re-training method can achieve better unlearning effects. Moreover, the unlearning effect of AlexNet is significantly better than ResNet18 in terms of  $AD_r$ . The effectiveness of the gradient ascent method varies for different datasets and models.

1) *Unlearning effectiveness of single-label unlearning:* On CIFAR-10, experimental results show that  $AD_f$  for re-training achieves 0, with an average  $AD_r$  reaching up to 92.77%. For gradient ascent,  $AD_f$  is around 7%, while the average  $AD_r$  stands at 51.09%. On Fashion-MNIST, the results demonstrate that  $AD_f$  for re-training also reaches 0, accompanied by an average  $AD_r$  of 95.27%. For gradient ascent,  $AD_f$  is approximately 3%, and the average  $AD_r$  is 83.4%.

In single-label unlearning, the gradient ascent method exhibits equally impressive performance when dealing with  $AD_f$ , effectively reducing or eliminating the memory of the specified label compared to re-training the model. However, its performance on  $AD_r$  is slightly worse, suggesting that the model may have slightly insufficient retention of other label knowledge. This indicates that while gradient ascent excels in unlearning specific labels, there is still room for improvement in maintaining the overall generalization ability of the model.

2) *Unlearning effectiveness of multi-label unlearning:* When  $\#C_f$  (i.e., the number of label categories to be unlearned) is set to 2, 4, and 7 across all models on CIFAR-10, the  $AD_f$  metric for re-training achieves 0, while the average  $AD_r$  metric reaches 94.08%. For gradient ascent, the  $AD_f$  metric stands at 6.64%, and the average  $AD_r$  metric is 48.77%. On Fashion-MNIST, experimental results show that the  $AD_f$  metric for re-training attains 0, with an average  $AD_r$  metric as high as 96.72%; the  $AD_f$  metric for gradient ascent is 1.64%, and the average  $AD_r$  metric is 61.1%.

Regarding the  $AD_f$ , the performance of gradient ascent is equally impressive compared to that of re-training the model. Regarding the  $AD_r$ , however, its performance exhibits a downward trend. This suggests that during optimization, the model’s emphasis on unlearned labels leads to insufficient or improper adjustments for retained labels, resulting in decreased performance on  $AD_r$  due to incomplete learning of relevant knowledge for these labels.

3) *Weight distance analysis:* We conduct an analysis of the ResNet18 model using the Fashion-MNIST dataset. In the presence of unlearned data ( $\#C_f = 1$ ), we evaluate the distance trend of the unlearning method. Additionally, we compute the layer-wise distances between the re-trained model and the original model, as well as between the gradient ascent method and the original model. We select the top-10 layer-wise examples. As shown in Fig. 5, the gradient ascent model has a similar trend to the re-trained model, proving the effectiveness of the gradient ascent method.

4) *Unlearning speed:* Experimental results demonstrated in Tables III and IV reveal that, while sequential unlearning with re-training offers more robust performance on unlearning effectiveness and retained model utility, parallel unlearning with gradient ascent is more efficient. On the CIFAR-10 dataset, as the number of inherited models increases, the cumulative time for unlearning using the gradient ascent method is reduced by a factor of 19, compared to the re-training method. Similarly, on the Fashion-MNIST, the gradient ascent method also demonstrates its efficiency, with an unlearning speed 12 times faster than re-training.

## F. Cost Evaluation

We analyze the time overhead of blockchain execution under the sequential paradigm with re-training and parallel paradigm with gradient ascent for the design goal G4. For each FL task, we establish a blockchain utilizing a single-chain structure. The network utilizes the BFT-based consensus mechanism. **Multi-model parallel update cost time.** For both re-training and gradient ascent methods, we analyze the blockchain overhead incurred when multiple models are executed in parallel.

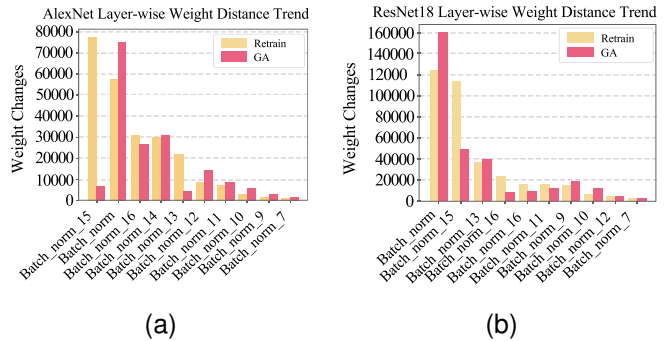


Fig. 5: The unlearned data category is  $\#C_f = 1$ . (a) and (b) depict the weight distances for ResNet18 on  $r_5$  and  $r_8$ , respectively.

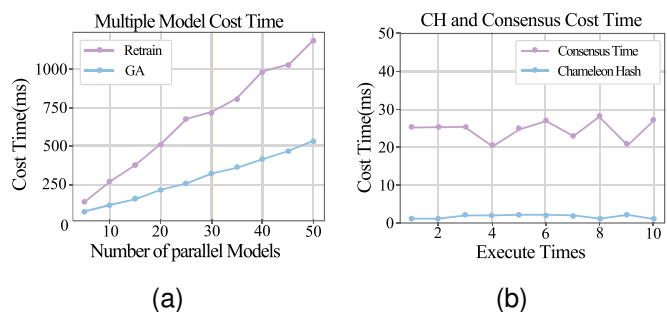


Fig. 6: (a) the cost time of multiple start models; (b) the cost time of a single start model.

We assume a DAG graph with only two models and the two models in different blocks, as illustrated in Fig. 6a. It is observed that both the re-training and gradient ascent methods demonstrate linear growth of the time overhead. This arises from the inherent competition for network and computational resources within the BFT-based consensus. The gradient ascent method incurs a maximum reduction of 124% in time overhead, compared to the re-training method.

**Chameleon hash and consensus cost time.** We conduct multiple trials to measure the CH and consensus computational overhead time for a single model, as illustrated in Fig. 6b. The execution time of CH and consensus remains consistently within a constant range. The consensus time is 92% longer than CH time, contributing to the majority of the blockchain time overhead.

**Tx-block cost time.** When a block contains a single transaction, we conduct experiments across multiple instances across different blocks. The horizontal axis indicates the number of transactions (the number of unlearning models), and the vertical axis gives the time cost. The results are illustrated in Fig. 7a, where we observe a linear growth in time consumption as the number of inheritance models increases for both methods. Compared to re-training, gradient ascent achieves a performance improvement of up to 75.8%.

**Txs-block cost time.** When a block contains multiple transactions, our experiments, aligned with (24) and depicted in Fig. 7b, reveal that the time consumption for both methods in-

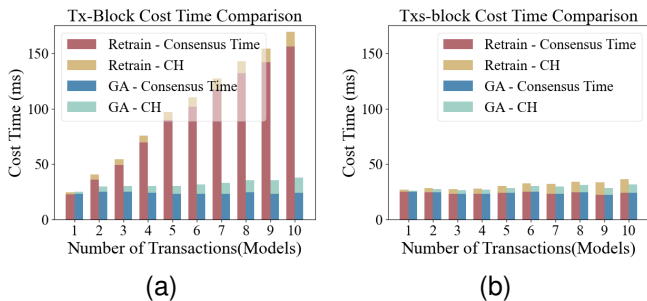


Fig. 7: (a) the cost time of multiple blocks of inheritance models; (b) the cost time of a single block of inheritance model.

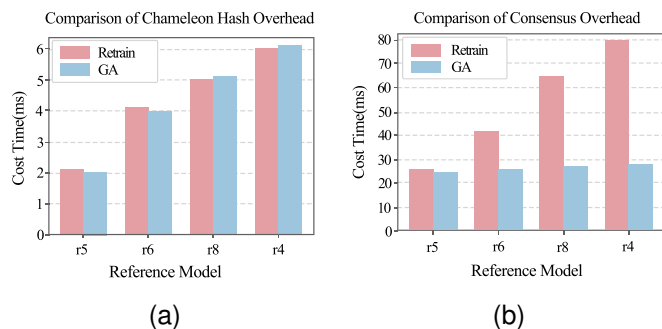


Fig. 8: (a) represents chameleon hash cost time; (b) represents consensus cost time.

creases linearly with the number of inherited models. However, the rate of increase is slower compared to the scenario shown in Fig. 7a, where transactions are packed in different blocks. The improvements in time efficiency are notable, reaching up to 4.4% and 12.6% for the re-training and gradient ascent methods, respectively. This is due to the overhead incurred by multiple block updates. The gradient ascent method achieves an improvement of up to 78.1% compared to re-training. This is attributed to the fact that the parallel paradigm only needs consensus once, whereas the sequential paradigm imposes substantial overhead with every model update from the client, owing to the consensus requirement.

**Chameleon hash overhead.** We assess the computational overhead of CH on the live chain, modifying the hash values of model *URI* for nodes  $r_4$ ,  $r_5$ ,  $r_6$ , and  $r_8$  as structured in Fig. 4. Each transaction aligns with one block as defined by (19), with  $K = N = 4$ . As shown in Fig. 8a, the modification time for each node is brief and falls within an acceptable range. The computational overhead increases linearly with the number of references, and the costs of both methods are comparable.

**Blockchain consensus overhead.** We conduct experiments employing the BFT-based consensus on the DAG structure illustrated in Fig. 4, as demonstrated in Fig. 8b. For the re-training method, our experiments reveal that the time required also rises as the reference number increases. However, for gradient ascent, we only need to conduct consensus once, so the overhead does not increase with the reference count. Notably, in comparison to the CH overhead, the consensus

overhead dominates in the majority of the cases. Thus, we have the flexibility to choose different consensus algorithms based on security and efficiency requirements.

## VII. CONCLUSION

In response to **RQ1** on how Blockchain FL frameworks can unlearn historical models while reducing the costs of updating multiple inherited models, we developed a new framework termed BlockFUL, which employs a dual-chain structure to enable traceable and trustworthy unlearning capability in BLockchained FL. To tackle **RQ2** regarding adaptable unlearning methods for Blockchain FL, we presented two paradigms under the BlockFUL framework: parallel and sequential unlearning, utilizing the prevalent unlearning methods of gradient ascent and re-training for demonstration. Our analysis revealed that parallel unlearning with gradient ascent is more cost-effective than sequential unlearning, particularly in consensus and transmission costs, as the number of model updates increases. Our experimental results demonstrated that sequential unlearning with re-training maintains high accuracy for retained data, while the effectiveness of parallel unlearning varies with inheritance depth and model differences.

## REFERENCES

- [1] M. Shayan, C. Fung, C. J. Yoon, and I. Beschastnikh, "Biscotti: A blockchain system for private and secure federated learning," *IEEE Transactions on Parallel and Distributed Systems*, vol. 32, no. 7, pp. 1513–1525, 2020.
- [2] T. Krauß, J. König, A. Dmitrienko, and C. Kanzow, "Automatic adversarial adaptation for stealthy poisoning attacks in federated learning," NDSS, 2024.
- [3] T. Li, A. K. Sahu, M. Zaheer, M. Sanjabi, A. Talwalkar, and V. Smith, "Federated optimization in heterogeneous networks," *Proceedings of Machine learning and systems*, vol. 2, pp. 429–450, 2020.
- [4] Y.-W. Chu, S. Hosseinalipour, E. Tenorio, L. Cruz, K. Douglas, A. S. Lan, and C. G. Brinton, "Multi-layer personalized federated learning for mitigating biases in student predictive analytics," *IEEE Transactions on Emerging Topics in Computing*, 2024.
- [5] Q. Li, Z. Wen, Z. Wu, S. Hu, N. Wang, Y. Li, X. Liu, and B. He, "A survey on federated learning systems: Vision, hype and reality for data privacy and protection," *IEEE Transactions on Knowledge and Data Engineering*, vol. 35, no. 4, pp. 3347–3366, 2021.
- [6] D. C. Nguyen, S. Hosseinalipour, D. J. Love, P. N. Pathirana, and C. G. Brinton, "Latency optimization for blockchain-empowered federated learning in multi-server edge computing," *IEEE Journal on Selected Areas in Communications*, vol. 40, no. 12, pp. 3373–3390, 2022.
- [7] Z. Qu, X. Li, J. Xu, B. Tang, Z. Lu, and Y. Liu, "On the convergence of multi-server federated learning with overlapping area," *IEEE Transactions on Mobile Computing*, vol. 22, no. 11, pp. 6647–6662, 2022.
- [8] C. Che, X. Li, C. Chen, X. He, and Z. Zheng, "A decentralized federated learning framework via committee mechanism with convergence guarantee," *IEEE Transactions on Parallel and Distributed Systems*, vol. 33, no. 12, pp. 4783–4800, 2022.
- [9] A. G. Roy, S. Siddiqui, S. Pölsterl, N. Navab, and C. Wachinger, "Braitentor: A peer-to-peer environment for decentralized federated learning," *arXiv preprint arXiv:1905.06731*, 2019.
- [10] E. T. M. Beltrán, M. Q. Pérez, P. M. S. Sánchez, S. L. Bernal, G. Bovet, M. G. Pérez, G. M. Pérez, and A. H. Celdrán, "Decentralized federated learning: Fundamentals, state of the art, frameworks, trends, and challenges," *IEEE Communications Surveys & Tutorials*, 2023.
- [11] Y. Jiang, B. Ma, X. Wang, G. Yu, P. Yu, Z. Wang, W. Ni, and R. P. Liu, "Blockchain federated learning for internet of things: A comprehensive survey," *ACM Computing Surveys*, vol. 56, no. 10, pp. 1–37, 2024.
- [12] Y. Qu, M. P. Uddin, C. Gan, Y. Xiang, L. Gao, and J. Yearwood, "Blockchain-enabled federated learning: A survey," *ACM Computing Surveys*, vol. 55, no. 4, pp. 1–35, 2022.

- [13] J. Zhu, J. Cao, D. Saxena, S. Jiang, and H. Ferradi, "Blockchain-empowered federated learning: Challenges, solutions, and future directions," *ACM Computing Surveys*, vol. 55, no. 11, pp. 1–31, 2023.
- [14] Y. Li, C. Chen, N. Liu, H. Huang, Z. Zheng, and Q. Yan, "A blockchain-based decentralized federated learning framework with committee consensus," *IEEE Network*, vol. 35, no. 1, pp. 234–241, 2020.
- [15] Z. Wang and Q. Hu, "Blockchain-based federated learning: A comprehensive survey," *arXiv preprint arXiv:2110.02182*, 2021.
- [16] L. Feng, Y. Zhao, S. Guo, X. Qiu, W. Li, and P. Yu, "Baf1: A blockchain-based asynchronous federated learning framework," *IEEE Transactions on Computers*, vol. 71, no. 5, pp. 1092–1103, 2021.
- [17] M. Uddin, K. Salah, R. Jayaraman, S. Pesic, and S. Ellahham, "Blockchain for drug traceability: Architectures and open challenges," *Health informatics journal*, vol. 27, no. 2, p. 14604582211011228, 2021.
- [18] S. S. Kamble, A. Gunasekaran, and R. Sharma, "Modeling the blockchain enabled traceability in agriculture supply chain," *International Journal of Information Management*, vol. 52, p. 101967, 2020.
- [19] K. Demestichas, N. Peppas, T. Alexakis, and E. Adamopoulou, "Blockchain in agriculture traceability systems: A review," *Applied Sciences*, vol. 10, no. 12, p. 4113, 2020.
- [20] A. Halimi, S. Kadhe, A. Rawat, and N. Baracaldo, "Federated unlearning: How to efficiently erase a client in fl?" *arXiv preprint arXiv:2207.05521*, 2022.
- [21] W. Yuan, H. Yin, F. Wu, S. Zhang, T. He, and H. Wang, "Federated unlearning for on-device recommendation," in *Proceedings of the Sixteenth ACM International Conference on Web Search and Data Mining*, 2023, pp. 393–401.
- [22] L. Bourtole, V. Chandrasekaran *et al.*, "Machine unlearning," in *2021 IEEE Symposium on Security and Privacy (SP)*. IEEE, 2021, pp. 141–159.
- [23] T. T. Nguyen, T. T. Huynh, P. L. Nguyen, A. W.-C. Liew, H. Yin, and Q. V. H. Nguyen, "A survey of machine unlearning," *arXiv preprint arXiv:2209.02299*, 2022.
- [24] A. Thudi, H. Jia, I. Shumailov, and N. Papernot, "On the necessity of auditable algorithmic definitions for machine unlearning," in *31st USENIX Security Symposium (USENIX Security 22)*, 2022, pp. 4007–4022.
- [25] V. S. Chundawat, A. K. Tarun, M. Mandal, and M. Kankanhalli, "Zero-shot machine unlearning," *IEEE Transactions on Information Forensics and Security*, 2023.
- [26] M. Chen, Z. Zhang, T. Wang, M. Backes, M. Humbert, and Y. Zhang, "When machine unlearning jeopardizes privacy," in *Proceedings of the 2021 ACM SIGSAC conference on computer and communications security*, 2021, pp. 896–911.
- [27] G. Yu, X. Zha, X. Wang, W. Ni, K. Yu, P. Yu, J. A. Zhang, R. P. Liu, and Y. J. Guo, "Enabling attribute revocation for fine-grained access control in blockchain-iot systems," *IEEE Transactions on Engineering Management*, vol. 67, no. 4, pp. 1213–1230, 2020.
- [28] J. Wei, Q. Zhu, Q. Li, L. Nie, Z. Shen, K.-K. R. Choo, and K. Yu, "A redactable blockchain framework for secure federated learning in industrial internet of things," *IEEE Internet of Things Journal*, vol. 9, no. 18, pp. 17901–17911, 2022.
- [29] Y. Jia, S.-F. Sun, Y. Zhang, Z. Liu, and D. Gu, "Redactable blockchain supporting supervision and self-management," in *Proceedings of the 2021 ACM Asia Conference on Computer and Communications Security*, 2021, pp. 844–858.
- [30] K. Huang, X. Zhang, Y. Mu, X. Wang, G. Yang, X. Du, F. Rezaeibagha, Q. Xia, and M. Guizani, "Building redactable consortium blockchain for industrial internet-of-things," *IEEE Transactions on Industrial Informatics*, vol. 15, no. 6, pp. 3670–3679, 2019.
- [31] J. Xu, K. Xue, H. Tian, J. Hong, D. S. Wei, and P. Hong, "An identity management and authentication scheme based on redactable blockchain for mobile networks," *IEEE Transactions on Vehicular Technology*, vol. 69, no. 6, pp. 6688–6698, 2020.
- [32] M. Chen, Z. Zhang, T. Wang, M. Backes, M. Humbert, and Y. Zhang, "Graph unlearning," in *Proceedings of the 2022 ACM SIGSAC conference on computer and communications security*, 2022, pp. 499–513.
- [33] M. Du, Z. Chen, C. Liu, R. Oak, and D. Song, "Lifelong anomaly detection through unlearning," in *Proceedings of the 2019 ACM SIGSAC conference on computer and communications security*, 2019, pp. 1283–1297.
- [34] K. Koch and M. Soll, "No matter how you slice it: Machine unlearning with sisa comes at the expense of minority classes," in *2023 IEEE Conference on Secure and Trustworthy Machine Learning (SaTML)*. IEEE, 2023, pp. 622–637.
- [35] W. Wu, L. He, W. Lin, R. Mao, C. Maple, and S. Jarvis, "Safa: A semi-asynchronous protocol for fast federated learning with low overhead," *IEEE Transactions on Computers*, vol. 70, no. 5, pp. 655–668, 2020.
- [36] S. Yuan, B. Cao, M. Peng, and Y. Sun, "Chainsfl: Blockchain-driven federated learning from design to realization," in *2021 IEEE Wireless Communications and Networking Conference (WCNC)*. IEEE, 2021, pp. 1–6.
- [37] G. Liu, X. Ma, Y. Yang, C. Wang, and J. Liu, "Federated unlearning," *arXiv preprint arXiv:2012.13891*, 2020.
- [38] Y. Cao and J. Yang, "Towards making systems forget with machine unlearning," in *2015 IEEE Symposium on Security and Privacy*. IEEE, 2015, pp. 463–480.
- [39] C. Chen, F. Sun, M. Zhang, and B. Ding, "Recommendation unlearning," in *Proceedings of the ACM Web Conference 2022*, 2022, pp. 2768–2777.
- [40] H. Yan, X. Li, Z. Guo, H. Li, F. Li, and X. Lin, "Arcane: An efficient architecture for exact machine unlearning," in *Proceedings of the Thirty-First International Joint Conference on Artificial Intelligence, IJCAI-22*, 2022, pp. 4006–4013.
- [41] Y. Liu, L. Xu, X. Yuan, C. Wang, and B. Li, "The right to be forgotten in federated learning: An efficient realization with rapid retraining," in *IEEE INFOCOM 2022-IEEE Conference on Computer Communications*. IEEE, 2022, pp. 1749–1758.
- [42] Y. Liu, M. Fan, C. Chen, X. Liu, Z. Ma, L. Wang, and J. Ma, "Backdoor defense with machine unlearning," in *IEEE INFOCOM 2022-IEEE Conference on Computer Communications*. IEEE, 2022, pp. 280–289.
- [43] C. Wu, S. Zhu, and P. Mitra, "Federated unlearning with knowledge distillation," *arXiv preprint arXiv:2201.09441*, 2022.
- [44] A. Golatkar, A. Achille, and S. Soatto, "Eternal sunshine of the spotless net: Selective forgetting in deep networks," in *Proceedings of the IEEE/CVF Conference on Computer Vision and Pattern Recognition*, 2020, pp. 9304–9312.
- [45] M. Jia, J. Chen, K. He, R. Du, L. Zheng, M. Lai, D. Wang, and F. Liu, "Redactable blockchain from decentralized chameleon hash functions," *IEEE Transactions on Information Forensics and Security*, vol. 17, pp. 2771–2783, 2022.
- [46] Y. Tian, N. Li, Y. Li, P. Szalachowski, and J. Zhou, "Policy-based chameleon hash for blockchain rewriting with black-box accountability," in *Proceedings of the 36th Annual Computer Security Applications Conference*, 2020, pp. 813–828.
- [47] L. Wu, S. Guo, J. Wang, Z. Hong, J. Zhang, and Y. Ding, "Federated unlearning: Guarantee the right of clients to forget," *IEEE Network*, vol. 36, no. 5, pp. 129–135, 2022.
- [48] N. Su and B. Li, "Asynchronous federated unlearning," in *IEEE INFOCOM 2023-IEEE Conference on Computer Communications*. IEEE, 2023, pp. 1–10.
- [49] T. Che, Y. Zhou, Z. Zhang, L. Lyu, J. Liu, D. Yan, D. Dou, and J. Huan, "Fast federated machine unlearning with nonlinear functional theory," in *International conference on machine learning*. PMLR, 2023, pp. 4241–4268.
- [50] J. Wang, S. Guo, X. Xie, and H. Qi, "Federated unlearning via class-discriminative pruning," in *Proceedings of the ACM Web Conference 2022*, 2022, pp. 622–632.
- [51] G. Yu, X. Wang, C. Sun, Q. Wang, P. Yu, W. Ni, and R. P. Liu, "Ironforge: An open, secure, fair, decentralized federated learning," *IEEE Transactions on Neural Networks and Learning Systems*, 2023.
- [52] P. Voigt and A. Von dem Bussche, "The eu general data protection regulation (gdpr)," *A Practical Guide, 1st Ed., Cham: Springer International Publishing*, vol. 10, no. 3152676, pp. 10–5555, 2017.
- [53] Y. Zhu, Y. Cheng, H. Zhou, and Y. Lu, "Hermes attack: Steal DNN models with lossless inference accuracy," in *30th USENIX Security Symposium (USENIX Security 21)*, 2021.
- [54] S. Rezaei and X. Liu, "On the difficulty of membership inference attacks," in *Proceedings of the IEEE/CVF Conference on Computer Vision and Pattern Recognition*, 2021, pp. 7892–7900.
- [55] G. Yu, X. Wang, K. Yu, W. Ni, J. A. Zhang, and R. P. Liu, "Survey: Sharding in blockchains," *IEEE Access*, vol. 8, pp. 14 155–14 181, 2020.
- [56] L. Wu, S. Guo, J. Wang, Z. Hong, J. Zhang, and Y. Ding, "Federated unlearning: Guarantee the right of clients to forget," *IEEE Network*, vol. 36, no. 5, pp. 129–135, 2022.
- [57] A. K. Tarun, V. S. Chundawat, M. Mandal, and M. Kankanhalli, "Fast yet effective machine unlearning," *IEEE Transactions on Neural Networks and Learning Systems*, 2023.
- [58] H. Kim, S. Lee, and S. S. Woo, "Layer attack unlearning: Fast and accurate machine unlearning via layer level attack and knowledge distillation," in *Proceedings of the AAAI Conference on Artificial Intelligence*, vol. 38, no. 19, 2024, pp. 21 241–21 248.